CSIRO PUBLISHING

Australian Journal of Physics

Volume 52, 1999

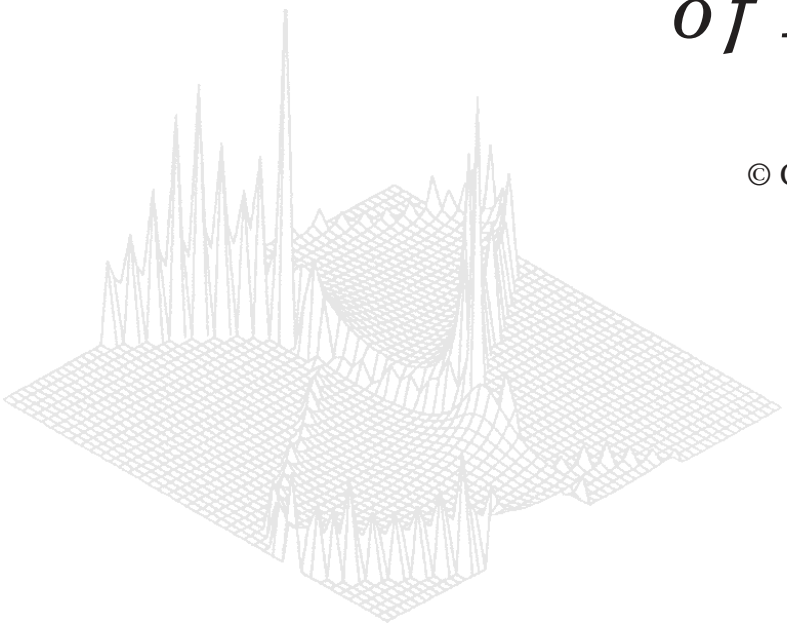

A journal for the publication of
original research in all branches of physics

www.publish.csiro.au/journals/ajp

All enquiries and manuscripts should be directed to
Australian Journal of Physics
CSIRO PUBLISHING
PO Box 1139 (150 Oxford St)
Collingwood Telephone: 61 3 9662 7626
Vic. 3066 Facsimile: 61 3 9662 7611
Australia Email: peter.robertson@publish.csiro.au

Published by **CSIRO** PUBLISHING
for CSIRO Australia and
the Australian Academy of Science

Aust. J. Phys., 1999, **52**, 27–36

Fibre Optic Shock Velocity Sensor for Solids

Jakub Szajman,[A] *Frank Di Marzio*[A,C] *and Michael Podlesak*[B]

[A]School of Communications and Informatics, Victoria University of Technology (F119), PO Box 14428, Melbourne City MC, Vic. 3001, Australia.
[B]Maritime Platforms Division, Aeronautical and Maritime Research Laboratory, Defense Science and Technology Organization, PO Box 3441, Melbourne, Vic. 3001, Australia.
[C]Present address: Trinity Education Centre, Trinity College, Royal Parade, Parkville, Vic. 3052, Australia.

Abstract

This paper reports a fibre optic sensing technique for the measurement of shock velocity in solid materials. The shock-induced changes in the light transmission properties of an optical fibre are employed as the principal transduction mechanism. A polycarbonate flyer plate generated shock waves by impacting a perspex target. The shock velocity was determined from the difference in arrival times of the shock front at the spatially separated optical fibres embedded in the target. The main advantage of this sensor system lies in its simplicity and immunity to optical and radio frequency (RF) noise. Consideration is also given to the effect of release waves on the uniform shock pressure region generated by the flyer impact which can degrade the accuracy of the velocity measurement.

1. Introduction

Previous investigations (Szajman *et al.* 1989*a*, 1989*b*; Podlesak 1992; Podlesak *et al.* 1993; Hatt and Ryan 1993) involving the design and characterisation of a large scale flyer plate generator, driven by an electrically exploded aluminium foil, have indicated that optical fibres may be employed to obtain flyer velocity information. Hence, the feasibility of applying a similar technique to the measurement of shock velocity in solid targets was examined. This paper reports the initial investigation of shock velocity measurements and some of the complicating effects such as the influence of release waves.

The flyer plate generator used in this study (Podlesak *et al.* 1993) is similar to the device described previously (Weingart *et al.* 1980). It utilises a hot, high-pressure metal vapour generated by an electrically exploded metal foil to propel a thin plastic plate towards a target sample. Upon impact, a uniform shock pressure region is generated both in the target as well as the flyer plate (Fig. 1). The forward propagating plane shock wave in the target is eroded by release waves initiated at the outer edge of the flyer plate while it is in contact with the target. A similar scenario applies to the backward propagating shock wave in the flyer plate.

 10.1071/PH98068 0004-9506/99/010027$05.00

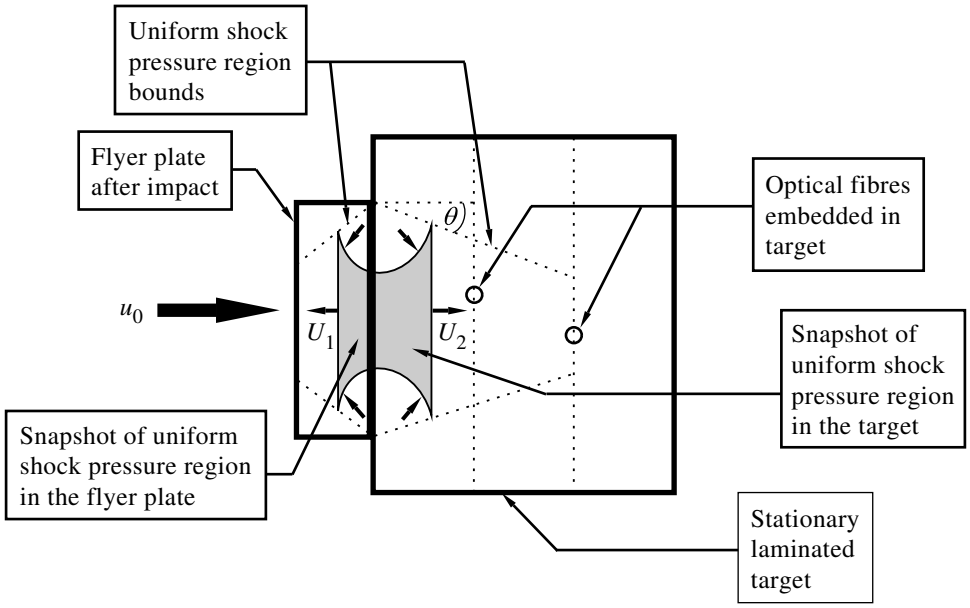

Fig. 1. Schematic diagram of shock pressure wave propagation in the flyer plate and target just after impact, where U_1 and U_2 are the respective shock wave velocities in the flyer and target and u_0 is the flyer velocity prior to impact. The angle θ defines the boundary of uniform shock pressure wave propagation through the target. The diagram is not to scale.

The shock wave velocity in a solid target has been measured by various means, including time of arrival gauges which can incorporate either an electric switch, piezoelectric or piezoresistive element, all of which give a distinct, rapid response output signal when subjected to an incident shock. The optical methods generally involve the use of high speed photography, flash X-ray radiography and piezo-luminescence (Duvall and Fowles 1963). It was found that when the large scale flyer generator (Podlesak 1992; Podlesak *et al.* 1993; Hatt and Ryan 1993) was used to produce shock waves in target samples, very large amounts of optical and RF noise were generated which had an adverse effect on measurement sensors and associated instrumentation. Fibre optic methods of sensing offer considerable immunity to this type of noise but, so far, the optical fibre has been used largely as a signal transmission device rather than as a sensor.

The technique used in this study is based on the principle of shock induced change in the light transmission properties of optical fibres embedded in a target. In the initial trials a He–Ne laser was employed to launch light into the fibres towards the detectors (Szajman *et al.* 1989*b*). It was assumed that the passage of shock through the fibre would cause a detectable modulation in the transmitted light amplitude due to the changes in the refraction index of the glass (hence, altering polarisation), fibre deformation or even fracture. However, the rapid deformation of the shocked fibre allowed an almost instantaneous entry of the strong ambient light generated by the hot gas driving the flyer plate into the fibre and overwhelmed the laser light. In the subsequent experiments, the entry of the external light into the fibre served as the optical signal marking the event (Di Marzio *et al.* 1995).

2. Experimental Method

The overall set-up of the large scale flyer plate generator has been described previously (Podlesak *et al*. 1993) and it was demonstrated that the fibre optic sensor can determine the flyer velocity accurately (Szajman *et al*. 1989*b*; Di Marzio *et al*. 1995). This technique was extended to measure shock velocity in solid targets and to characterise them in terms of shock velocity Hugoniots. The basic shock Hugoniot relations governing the propagation of these shock waves and the effect of the release waves in the flyer plate and the target are both outlined in the Appendix.

The flyer plates used in the experiments were made from the commercially cast sheet polycarbonate (Lexan) with dimensions $0{\cdot}5\,\text{mm}\times10\,\text{mm}\times10\,\text{mm}$. The flyer plate was accelerated by hot gases generated from the discharge of a large current through a thin aluminium foil. The target was positioned in such a way that the flyer reached maximum speed just before impact and the resultant shock waves were detected using the optical fibre system displayed in Fig. 2.

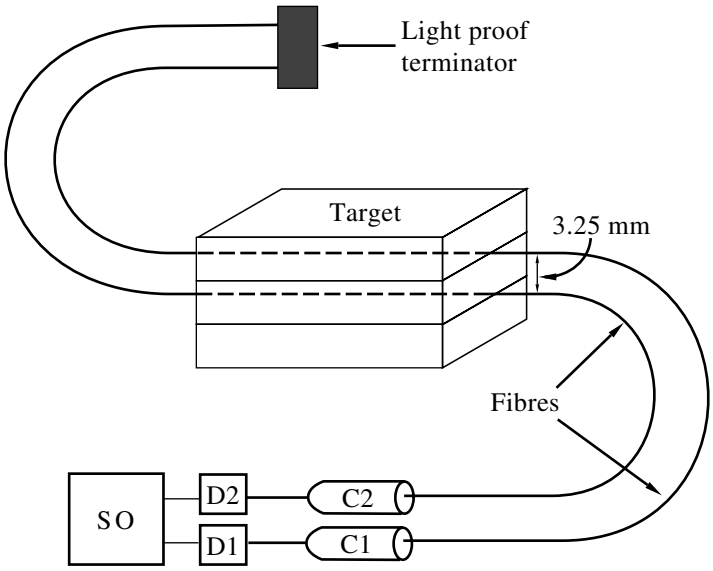

Fig. 2. Schematic diagram of the fibre optic sensor system used in the shock wave velocity studies. The signals detected by the optical fibres are registered by detectors D1 and D2 and recorded in a storage oscilloscope (SO). The pigtails are joined to the fibres using mechanical connectors C1 and C2.

In most experiments the optical fibres were sandwiched between three ($100\,\text{mm}\times100\,\text{mm}\times3\,\text{mm}$) perspex laminae. The fibres were $50/125\,\mu$m diameter multimode glass, encased within a $250\,\mu$m diameter acetate jacket. The fibres were embedded in such a way that there were no gaps between the target blocks so that the possibility of shock disruption by voids was minimised. In this configuration the fibre separation was $3{\cdot}25\,\text{mm}$.

In addition, the free ends of the optical fibres were covered to prevent stray light from entering and possibly confounding the results. The system was thus

based on the fact that as the shock wave deformed the fibres, the light emitted from the hot gases entered the fibres and was sensed by the optoelectronic converter. The electric output from the converter was recorded on a Tektronix 2240 dual channel digitising oscilloscope with 125 MHz single-shot bandwidth and 500 MSamples per second sampling rate per channel.

3. Results and Estimation of the Release Wave Effect

The firing voltage used in the experiments was fixed at 5 kV, generating a flyer velocity of $1{\cdot}5 \pm 0{\cdot}3\,\mathrm{km\,s^{-1}}$ for a 10 mm pre-launch stand-off between the flyer plate and the target face. During these experiments, flyer velocity was not measured, but inferred from the calibration data for the rig (Podlesak *et al.* 1993).

The results from these tests are given in Table 1, with the corresponding optical fibre output shown in Fig. 3. The arrival of the shock wave is evident from a rapid rise in the recorded waveform and yielded shock velocities of $3{\cdot}5\,\mathrm{km\,s^{-1}}$ and $3{\cdot}2\,\mathrm{km\,s^{-1}}$ respectively (Table 1). Although the spread in values is largely attributable to individual variations of flyer impact velocity, the measured shock velocity falls somewhat short of $3{\cdot}9\,\mathrm{km\,s^{-1}}$ based on published shock Hugoniot data (Table 2). The lower measured values suggest the possibility of shock attenuation due to rarefactions.

To estimate the effect of rarefaction waves, knowledge of the shock velocity Hugoniot constants C_0 and S in equation (A1) is required. Since the tests were

Table 1. Experimental data from fibre optic shock velocity measurements in a perspex target impacted by a polycarbonate flyer plate at $1{\cdot}5\,\mathrm{km\,s^{-1}}$

Data	Optical fibre separation (mm)	Shock arrival time difference (μs)	Average shock velocity ($\mathrm{km\,s^{-1}}$)
Fig. 3*a*	3·25	0·94	3·5
Fig. 3*b*	3·25	1·03	3·2
Fig. 4	3·25	0·84	3·9

Table 2. Published shock Hugoniot data and predicted shock velocity in perspex target impacted by a polycarbonate flyer plate at $1{\cdot}5\,\mathrm{km\,s^{-1}}$

The numbers in parentheses refer to the references cited by Deal (1965). The asterisk indicates an assumed density where no density value was provided

Material	C_0 ($\mathrm{km\,s^{-1}}$)	S	ρ ($\mathrm{kg\,m^{-3}}$)	U ($\mathrm{km\,s^{-1}}$)
Polycarbonate (Lexan)	2·75	1·48	1180	—
Plexiglass I	2·66	2·00	1178	4·1
Cast PMMA (2)	2·56	1·69	1180*	3·8
Plexiglass II, UVA (4,5)	2·68	1·61	1180	3·9
PMMA (8)	2·70	1·76	1180*	4·0
Perspex (11)	3·03	1·30	1180	4·0
Plexiglass (13)	2·74	1·53	1180	3·9
Perspex (17)	3·10	1·13	1180*	3·9
Average	2·78	1·56	1180	3·9

restricted to a one impact velocity value, C_0 and S could not be determined from the experimental data. However, an estimate of the Hugoniot constants was obtained from the published data for Lexan (polycarbonate) (Hull users manual 1987) and polymethyl methacrylate (PMMA) (Deal 1965), with the relevant information reproduced in Table 2. As pointed out by Deal a wide variation of shock parameters can exist between various batches of PMMA, depending on the method of production as well as purity of the chemical stock.

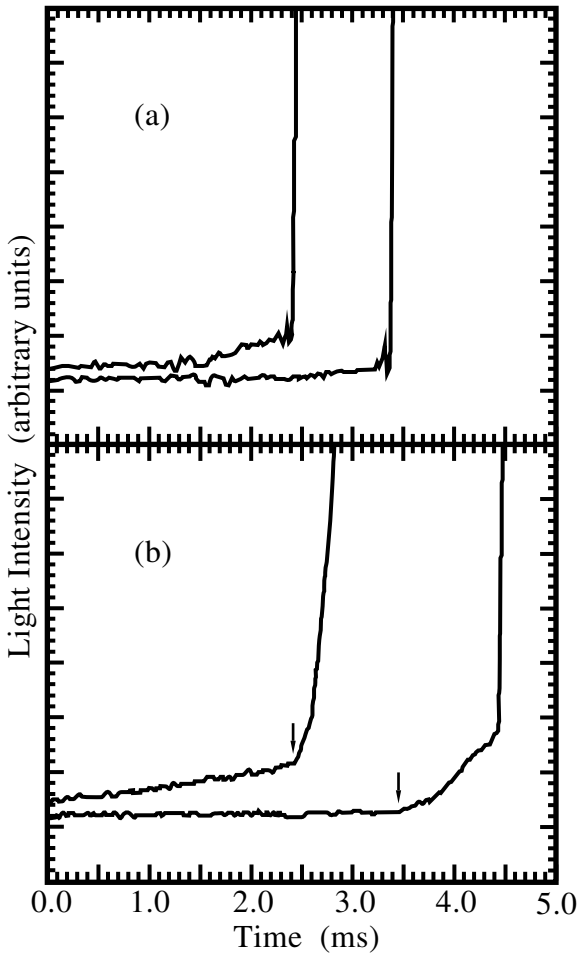

Fig. 3. (*a*) Shock response of optical fibres embedded in a perspex target. The onset of the steep rise for each trace is taken as the shock arrival time. (*b*) Another set of results revealing a much more distinct double gradient rise in both channels. The arrows indicate the time of shock arrival.

From Fig. 1 and (A9) the convergence angle of the uniform shock pressure boundary was found to be $\theta \approx 36°$. Since the flyer plate width was 10 mm, the uniform shock pressure region is estimated to extend to less than 7 mm into the target which is still sufficient to contain the optical fibres in these experiments.

It is also possible to avoid potential interference from release waves generated through shock wave interaction with the first fibre by laterally offsetting the second fibre by more than $4{\cdot}5\,\mathrm{mm}$.

The possibility of shock attenuation due to interference by the release waves generated at the rear free surface of the flyer plate is also considered (Fowles 1960). Neglecting lateral release wave effects, and with comparable shock Hugoniots for the flyer plate and the target, a value $x \approx 3{\cdot}5\,\mathrm{mm}$ was obtained from (A13). This indicates that the rarefaction wave emanating from the rear surface of the flyer plate catches up to the shock front at a position close to the first fibre and consequently it could reduce the measured shock velocity.

In a preliminary investigation of this effect, the first fibre was located on the impact face of the target and the second fibre placed $3{\cdot}25\,\mathrm{mm}$ behind it. Such a configuration should produce an increased value for the shock velocity because of the absence of release wave interference. Indeed, the result for this experimental arrangement, displayed in Fig. 4, yielded a shock velocity of $3{\cdot}9\,\mathrm{km\,s^{-1}}$ in excellent agreement with shock Hugoniot data indicating little, if any, interference from release waves.

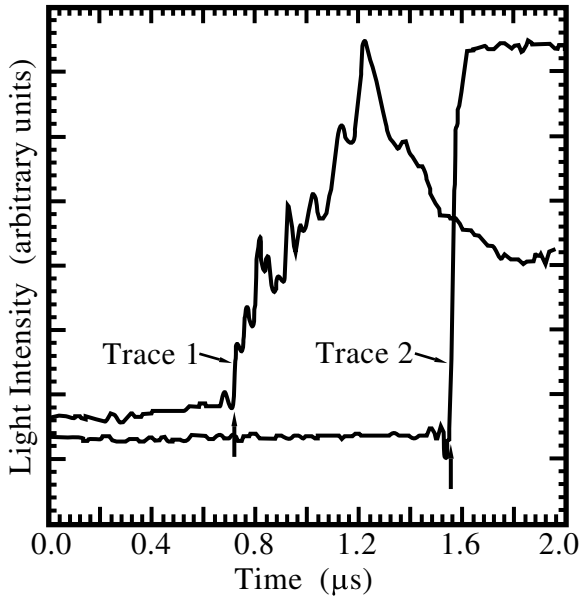

Fig. 4. Optical fibre response to shock with the first fibre placed on the impact face of the target and the second $3{\cdot}25\,\mathrm{mm}$ behind. Both fibres were laterally offset and the output of the first fibre was optically attenuated. The arrows indicate the time of shock arrival.

4. Discussion and Conclusions

Typical results for the shock wave velocity measurements are presented in Fig. 3. The sharp rise in the traces indicates shock-induced fracture of the fibres. Occasionally the optical fibres can also microbend prior to fracture and allow light to leak into the fibre leading to an initial slower increase in signal intensity before complete breakage as is evident in Fig. 3*b*.

For accurate timing of shock propagation the usual requirement is a distinct leading edge in the trace. This invariably results in the detectors being driven into saturation as displayed in Trace 2 of Fig. 4. The small ripple observed in the saturated region is attributable to electronic noise.

It is also interesting to observe the modulation of light intensity during the passage of the shock wave through the material. This was implemented by optically attenuating the signal from the first fibre (Trace 1, Fig. 4). Note that the leading edge of Trace 1 is just as sharp as that of Trace 2 but scaled down by approximately a factor of five by the attenuation. The features normally masked by the saturation of the optical detector are now discernible. The region prior to the leading edges in both traces is again due to electronic noise.

It is difficult to interpret the shape of the attenuated trace because of the numerous factors which could contribute to the variation in light levels. These may be due to localised heating in the fractured fibre (Veeser *et al*. 1987), variations in the index of refraction of the glass fibre, pressure induced changes in the opaqueness of the perspex, an indication of the fluctuations in the intrinsic brightness of the plasma, and/or variations associated with debris.

The experimental results obtained indicate that the optical fibre sensor system (particularly in the configuration designed to minimise release wave interference) may prove to be both a useful as well as inexpensive technique for shock velocity determinations in solids. The fibre sensor displays distinct shock response features and considerable immunity to electromagnetic interference, although its response has not been studied in opaque targets in which external light leakage does not contribute to the shock detection process. However, the reintroduction of He–Ne laser light through the fibres would be suited to such studies.

Some work is still required to establish the range, validity and accuracy of the technique. To this end there is a need for a positive identification of the underlying physical processes involved in the basic transduction mechanism which may be accomplished by utilising complementary measurement techniques such as high speed photography. The results obtained thus far are encouraging and it is expected that the technique will not only introduce an additional experimental tool, but may also lead towards the development of an inexpensive shock sensor immune to RF interference.

Acknowledgments

It is a pleasure to acknowledge fruitful discussions with Dr Alex Mazzolini.

References

Computational Mechanics Associates (1988). Explosive technology (course notes), Bethesda, Maryland, USA.

Deal, W. E. (1965). Shock wave research on inert solids. 4th Int. Symp. on Detonation, p. 321, Office of Naval Research Report ACR-126, USA.

Di Marzio, F., Szajman, J., and Mazzolini, A. (1995). *Aust. J. Phys.* **48**, 79.

Duvall, G. E., and Fowles, G. R. (1963). *In* 'High Pressure Physics and Chemistry', Vol. 2 (Ed. R. S. Bradley), Sect. 9, p. 209 (Academic: London).

Fowles, G. R. (1960). *J. Appl. Phys.* **31**, 655.

Hatt, D. J., and Ryan, P. F. X. (1993). Calibration and testing of a large-scale electric gun for shock Hugoniot measurements. Research Report MRL-TR-93–24(U), Materials Research Laboratory, Melbourne, Australia.

HULL users manual (1987). Orlando Technology Incorporated, Shalimar, Florida, p. II-V-6.
Podlesak, M. (1992). Breakwire technique for hypervelocity measurements, Technical Report MRL-TR-92–39(U), Materials Research Laboratory, Melbourne, Australia.
Podlesak, M., Richardson, D. D., and Olsson, C. (1993). An exploding foil flying plate generator for shock wave studies—calibrations, Research Report MRL-RR-1–92(U), Materials Research Laboratory, Melbourne, Australia.
Skidmore, I. C. (1965). *Appl. Mater. Res.* **4**, 131.
Szajman, J., Di Marzio, F., and Mazzolini, A. (1989*a*). The use of optical fibre sensors in the measurement of high velocity and shock waves, Technical Report L93069·7, Victoria University of Technology, Melbourne, Australia.
Szajman, J., Di Marzio, F., Mazzolini, A., and Podlesak, M. (1989*b*). Proc. Conf. of Australasian Instrumentation and Measurement, p. 14 (Inst. of Engineers: Adelaide).
Veeser, L. R., George, M. J., Menikoff, R., Papatheofanis, B., McGurn, J. S., and Gobby, P. L. (1987). *SPIE—Fibre Optic Laser Sensors V* **838**, 60.
Weingart, R. C., Jackson, R. K., Honodel, C. A., and Lee, R. S. (1980). *Propellants Explosives* **5**, 158.

Appendix: Shock Velocity Hugoniots and Release Wave Relations

The assumptions concerning shock propagation in solids follow mainly those given by Skidmore (1965). A shock propagating into a material of known state is completely specified by a knowledge of shock velocity U and particle velocity u, where other equation of state variables may be derived through the Rankine–Hugoniot relations. The shock velocity measurements are restricted to uniaxial strains only. The shock and particle velocities for a given phase in most solid materials (including many liquids) is given by the empirical relation (Skidmore 1965)

$$U = C_0 + Su\,, \tag{A1}$$

which applies over a wide range of pressures and where C_0 and S are constants. The average shock velocity U can be derived from time of arrival measurements using two staggered optical fibres.

The particle velocity can be obtained from the measurement of the free surface velocity of the rear target face which reaches a maximum of approximately twice the particle velocity during the shock rarefaction process. The technique used in this study derives u from the flyer plate impact velocity. For dissimilar materials, pressure–particle-velocity relations have to be used for the flyer and the target to solve for the respective particle velocities. This is given by a relation derived from conservation of mass and momentum across a shock front,

$$P = \rho_0 U u\,, \tag{A2}$$

where P is the pressure difference between the shocked and unshocked region, ρ_0 is the unshocked material density and the particle velocity of the unshocked material is assumed to be zero. At the impact interface, pressure and particle velocities are required to be continuous. Therefore, we have

$$\rho_1 U_1 u_1 = \rho_2 U_2 u_2\,, \tag{A3}$$

where subscripts 1 and 2 refer to the flyer and target materials respectively. Given that the target is stationary and the flyer has a pre-impact velocity u_0 and the

particle velocity at the interface is u, then basic kinematic considerations require

$$\begin{cases} u_1 = u_0 - u \\ u_2 = u \quad . \end{cases} \tag{A4}$$

Thus the shock velocity Hugoniot relations for the flyer and target material are

$$U_1 = C_1 + S_1(u_0 - u)\,, \tag{A5}$$

$$U_2 = C_2 + S_2 u\,. \tag{A6}$$

Substituting (A5) and (A6) into (A3) yields a quadratic equation with only one solution being physically meaningful, namely

$$u = \frac{-(C_1\rho_1 + C_2\rho_2 + 2\rho_1 S_1 u_0) + \mathcal{F}}{2(\rho_2 S_2 - \rho_1 S_1)}\,, \tag{A7}$$

where

$$\mathcal{F} = \sqrt{(C_1\rho_1 + C_2\rho_2 + 2\rho_1 S_1 u_0)^2 + 4\rho_1(\rho_2 S_2 - \rho_1 S_1)u_0(C_1 + S_1 u_0)}\,. \tag{A8}$$

If the same material is used for both the flyer plate and the target then the combination of (A4), (A5) and (A6) yields a linear equation in u whose solution is $u = u_0/2$. Hence, if the flyer plate is of the same material as the target, or if it is different but its shock Hugoniot is known, then the target material can be fully characterised by measuring flyer velocity and shock velocity in the target. However, two sets of independent data are required to solve for C_0 and S.

In practice it is not possible to perform experiments in a perfectly uniaxial environment because of the finite sizes of the flyer plate and target block. On impact, lateral release waves are generated at the edge of the flyer plate and target interface and will propagate into the uniformly shocked region. Release waves propagate faster than the shock front since sound velocity is higher in the shocked region (A10). Thus a convergent uniform shock pressure region is generated and this is indicated by the broken lines in Fig. 1. The duration of the shock pulse is ultimately limited by the thickness of the flyer plate because of the rarefaction wave generated at its free rear surface. The head of this wave propagates back towards the target at a speed greater than that of the shock and when it reaches it, the shock pressure front decays rapidly (Fowles 1960).

The convergence angle of the uniform shock pressure boundary θ is defined by (Computational Mechanics Associates 1988)

$$\tan^2\theta = \left(\frac{c}{U}\right)^2 - \left(\frac{U-u}{U}\right)^2\,, \tag{A9}$$

where c is the speed of the release wave in the shocked region and is related to shock pressure P and the shocked material density ρ by

$$c^2 = \frac{\partial P}{\partial \rho}\,. \tag{A10}$$

Using conservation of mass across the shock front, ρ is defined in terms of the other shock parameters as

$$\rho(U-u) = \rho_0 U\,. \tag{A11}$$

Equation (A10) can be expressed in terms of shock velocity Hugoniot parameters by using (A1), (A2) and (A11), giving

$$c^2 = \left(1 + \frac{2S}{C_0}u\right)[C_0 + (S-1)u]^2\,. \tag{A12}$$

For uniaxial shock compression, the distance x traversed by the shock wave front in the target before it is caught up by the release wave generated at the rear free surface of the flyer plate is determined from

$$\frac{d}{U_1} + \frac{d}{c_1}\left(1 - \frac{u_1}{U_1}\right) + \frac{x}{c_2}\left(1 - \frac{u_2}{U_2}\right) \approx \frac{x}{U_2}\,, \tag{A13}$$

where d is the thickness of the flyer and c_1 and c_2 are the respective release wave velocities in the flyer plate and target. The terms in brackets account for the shock compression of the flyer and target materials according to (A11).

Manuscript received 14 September, accepted 23 November 1998